AstroPix: Novel monolithic active pixel silicon sensors for future gamma-ray telescopes

Amanda L. Steinhebel[a,b], Henrike Fleischhack[c,b,d], Nicolas Striebig[e], Manoj Jadhav[f], Yusuke Suda[g], Ricardo Luz[f], Carolyn Kierans[b], Regina Caputo[b], Hiroyasu Tajima[h], Richard Leys[e], Ivan Peric[e], Jessica Metcalfe[f], and Jeremy S. Perkins[b]

[a]NASA Postdoctoral Program Fellow
[b]NASA Goddard Space Flight Center, Greenbelt, MD, USA
[c]Catholic University of America, Washington, DC, USA
[d]Center for Research and Exploration in Space Science and Technology, NASA/GSFC, Greenbelt, MD, USA
[e]Karlsruhe Institute of Technology, Karlsruhe, Germany
[f]Argonne National Laboratory, Lemont, IL, USA
[g]Hiroshima University, Higashi-Hiroshima City, Hiroshima, Japan
[h]Institute for Space-Environment Research, Nagoya University, Nagoya, Aichi, Japan

ABSTRACT

Space-based γ-ray telescopes such as the *Fermi* Large Area Telescope have used single sided silicon strip detectors to track secondary charged particles produced by primary γ-rays with high resolution. At the lower energies targeted by keV-MeV telescopes, two dimensional position information within a single detector is required for event reconstruction - especially in the Compton regime. This work describes the development of monolithic CMOS active pixel silicon sensors – AstroPix – as a novel technology for use in future γ-ray telescopes. Based upon sensors (ATLASPix) designed for use in the ATLAS detector at the Large Hadron Collider, AstroPix has the potential to maintain high performance while reducing noise with low power consumption. This is achieved with the dual detection and readout capabilities in each CMOS pixel. The status of AstroPix development and testing, as well as outlook for future testing and application, will be presented.

Keywords: AstroPix, silicon pixel detectors, Compton telescopes, MAPS, high energy astrophysics

1. INTRODUCTION

The modern era of multi-messenger astronomy requires that many cosmic messengers be monitored, including the full electromagnetic spectrum. The 'MeV Gap' in instrument sensitivity to γ-rays in the keV-MeV range must be addressed to allow input to multi-messenger investigations in this regime. In order to ensure high precision and sensitivity, a next-generation Pair/Compton telescope targeting the MeV γ-ray sky requires detectors with high energy and position resolution in three-dimensions, as well as a low energy threshold. The technology used to track the paths of secondary charged particles resultant of incident γ-rays in currently flying γ-ray telescopes such as single- and double-sided silicon strips cannot easily meet these challenges - the long strips introduce noise which impacts the measurement (see Ref 1). Instead, Complementary Metal-Oxide-Semiconductor (CMOS) monolithic active pixel silicon (MAPS) sensors can be used.

Individual pixels on these sensors can a range in size from 10 μm^2 - 1 mm^2, allowing for great control over position resolution (though this must be optimized with respect to power draw and data rate). The use of in-pixel CMOS circuitry (see Ref. 2) eliminates the necessity for an external ASIC to record and digitize data as the charge collection and digitization is all done on-chip. A CMOS chip (see Fig. 1) incorporates charge collection, signal amplification, and a comparator for signal acceptance in a shared substrate embedded directly
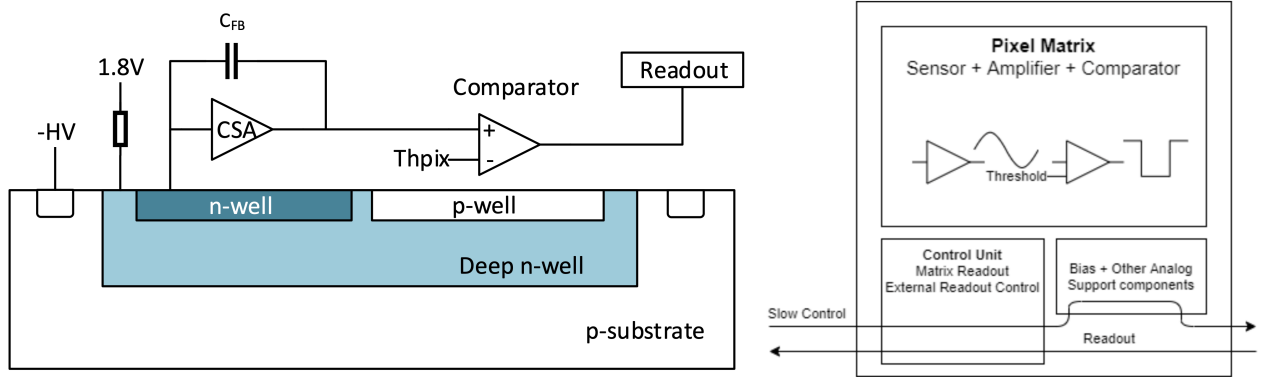

Figure 1: Illustration of an HVMAPS CMOS pixel with HV bias voltage (left) containing charge collection and amplification/comparator architecture embedded in the pixel matrix (figure from 4). This matrix reads out to a control unit on the digital periphery (right) for digitization and chip readout.

into the pixel matrix in shallow wells. The wells are isolated from the bulk substrate by a deep n-well. A charge-depleting bias voltage is applied individually to every pixel allowing for faster and more complete charge collection as compared to sensors that rely on diffusion. This makes AstroPix an HVMAPS sensor - MAPS that are depleted with high-voltage (HV) ($\mathcal{O}(100V)$) at a pixel level.

The comparator output for every pixel is sent to the synthesized digital logic which is located on the periphery of the chip. Here, the signal is digitized and can be read out for analysis. In this way, there is no need to directly bump-bond to each pixel to achieve high position resolution (as done with hybrid technology) as this strategy would introduce passive material into the active area of the detector. Large detectors designed with silicon strips require daisy-chaining the strips together, but the lack of this daisy-chaining with a HVMAPS sensor reduces capacitance and therefore noise in the signal. The AstroPix data collection strategy aims to reduce per-pixel power and overall data bandwidth. To this end, the comparator outputs for each row and column are OR'ed together and these two channels are sent to the digital periphery. In this way, the output signal is similar to the output of a silicon strip-based detector and row/column pairing algorithms will be employed to determine which signals correspond to which interaction if there are multiple triggers in a chip. Currently, AstroPix utilizes SPI readout from a DAQ which interfaces with an FPGA.

CMOS technology is familiar to industry and commercial endeavors, but novel in this application for space-based telescopes. AstroPix is a CMOS HVMAPS under design for this explicit purpose. The design of AstroPix is based upon work previously conducted by the ATLAS Collaboration at the Large Hadron Collider (LHC) for the development of an upgrade to their inner tracker subdetector system (see Ref. 3). This custom MAPS detector, ATLASPix, was designed for the LHC environment - optimized for minimum ionizing particles with nanosecond timing capability.

The AstroPix design philosophy utilizes ATLASPix as a starting point, and involves a sequence of AstroPix versions in order to advance the design in steps from ATLASPix to a flight-ready AstroPix. These versions are denoted with an underscored _v. This strategy ensures functional chips at each stage of testing. With continued optimization and characterization studies such as those outlined in this work, AstroPix can serve as a baseline detector for future telescope concepts - especially those that require high-resolution and low-noise/low-power electronics or those targeting the keV-MeV γ-ray regime. For more background information about detection strategies of keV-MeV γ-rays and its impact on telescope design, see Ref. 1.

Section 2 outlines the first changes made to ATLASPix to produce a $bona-fide$ AstroPix chip, AstroPix_v1. This section overviews the characterization effort of this sensor, including analysis of analog data, background estimation, and the creation of a calibration curve. Following the design strategy of incremental changes, AstroPix_v1 was superseded by AstroPix_v2 - the current design under testing. Section 3 mirrors the structure of Section 2 with the updated sensor. AstroPix_v2 was exposed to multiple particle beams and underwent preliminary radiation testing which is discussed in Section 4. Section 5 outlines plans for the next version of AstroPix,

Table 1: Parameters of ATLASPix and AstroPix.

	ATLASPix (Measured)	AstroPix (Required)
Sampling rate [ns]	16	~ 600
$E_{res.}$ (FWHM)	7% at 30.1 keV	9.7% at 122 keV
Pixel size [μm]	150$\times$50	1000×1000
Thickness [μm]	100	500
Dynamic range [keV]	5-32	25-700
Power consumption [mW/cm^2]	150	1.5

AstroPix_v3, and environmental testing plans. It also contains a general outlook and summary.

2. ASTROPIX_V1

The feasibility of using ATLASPix as a technological starting point for AstroPix was directly tested at NASA Goddard Space Flight Center (GSFC) in Ref. 1 where the measured energy resolution was found to be 7.69$\pm$0.13% at 5.89 keV and 7.27$\pm$1.18% at 30.1 keV. Analog recorded data (response pulses as measured from one pixel) was used for this measurement. Digital data (bitstreams with encoded hit information from the full array) was also considered, but individual pixel responses were untuned resulting in large spreads in the Gaussian-fit response distribution (up to $\sigma/\mu = 60\%$) when considering the summed response of the array as a whole.

Testing and characterization of the first AstroPix version, AstroPix_v1, has been completed and is presented in this section. Like ATLASPix, both analog data and digital data will be collected from AstroPix. Although digital data is intended to be utilized in flight, preliminary analog data is the focus of AstroPix_v1 studies as digital data readout was not available in AstroPix_v1 due to a flaw in the chip design. Missing shielding allowed parasitic capacitance to induce feedback and cause oscillations in the comparators. These oscillations were reproducible in simulation and are considered understood. All subsequent versions of the chip correct this defect.

Unless otherwise specified, the energy resolution is defined as the ratio of full width at half maximum (FWHM) of the reconstructed energy distribution over the mean of the reconstructed energy, expressed as a percent. The reconstructed energy spectrum for a mono-energetic input is assumed to follow a Gaussian shape, with mean μ and width σ. Thus, $E_{res} = 2.355 * |\sigma|/\mu * 100\%$.

2.1 Design Optimization for AstroPix_v1

The sensitivity of future γ-ray telescopes in the keV-GeV range is driven by the effective area, angular resolution, and energy resolution of the instrument. By using a thick wafer of at least 500 μm, AstroPix must measure energy resolution at FWHM of 5 keV from 25-122 keV and 5.6 keV at 622 keV with a pixel dynamic range of 25-700 keV. AstroPix pixel size is a compromise between position resolution and power consumption. Smaller pixels provide higher position resolution however an increased number of pixels causes increased data rates and higher overall power consumption.

ATLASPix provided a promising starting point, but itself does not meet telescope design criteria (see Table 1). From here, AstroPix_v1 was designed with 18 rows and columns of 175×175 μm pixels on an un-thinned 725 μm thick wafer. The wafer thickness enables the larger dynamic range desired by AstroPix, and larger pixels do not sacrifice energy resolution. Loosening the timing requirement from ATLASPix allows for a simpler readout system. In turn, noise-reducing components could be added on-chip. For example, the addition of a low pass filter after the charge amplifier allowed for improved energy resolution.

Figure 2: AstroPix_v1 mounted on a carrier board. A 3D-printed shield covers the chip with a layer of kapton to protect the wireboards.

2.2 AstroPix_v1 Testing Setup

AstroPix_v1 is controlled and configured by a Nexys Video FPGA and readout system adaptor (GECCO) board. Three extension boards are required, which enable 1) configuration, 2) voltage setting, and 3) the injection of a square analog transient signal for chip testing. AstroPix_v1 is mounted to a carrier board (see Fig. 2) using conductive pressure sensitive tape and then wire-bonded. This carrier board connects directly to the GECCO board through an PCIe slot. High-voltage reverse bias is supplied for charge depletion on a pixel-by-pixel basis.

Analog signals are displayed on a mixed domain oscilloscope. SMA ports on the injection card and output pixels are connected directly to the oscilloscope. Two AstroPix_v1 chips mounted to carrier boards were tested at GSFC and are considered in this work - Chip003 and Chip004. Each chip has 18 pixels connected to pads and capable of analog readout. Two pixels were chosen for the studies presented in this work - (1,18) or 'amp1' and (18,1) or 'amp2' indicates pixel (18,1). This provides two pixels in the corners of the array to avoid crosstalk. Known chip defects prohibit the use of the digital readout system, so all studies performed in the work will focus only on the analog signal detected in these two spatially separated pixels.

Response signals are read with a supplied bias voltage of -60V. This value is not optimized for full depletion, and as such it is not anticipated that AstroPix_v1 meets the full AstroPix design requirement of 500 μm depletion. With the 250 ± 50 $\Omega*$cm resistivity wafers used for AstroPix_v1, ithe depletion depth was estimated to 3-100 μm.

2.3 AstroPix_v1 Characterization Studies

2.3.1 Charge Injection Studies

AstroPix is designed along with the capability to receive an injected charge signal. This artificial signal is used as an initial test to confirm that correct configuration is successfully being passed to the AstroPix chip, and that analog and digital responses can be triggered upon and read out. The injected signal itself, a square wave with programmable frequency and duration can be observed with a digital oscilloscope. This injected pulse is used to trigger data collection upon the falling edge.

Using a bias voltage of -60 V, both pixels respond but with different pulse shapes. For chip003, amp1 reliably has lower pulse height and longer pulse duration than amp2. This in part is due to the shaping seen in amp1 with a more linear pulse decay rather than the more exponential nature seen in amp2. This behavior is opposite for chip004 (see Fig. 3) where amp1 showed much higher pulse heights than amp2. The linear or exponential nature of the pulse decay are consistent between amp1 and amp2 of the different chips. This leads to a pulse duration for amp1 of both chips of around 600 μs compared to 300 μs for amp2. As this analog signal is readout from the chip prior to digitization, the differences in pulse shape are related to the variability of amplification and shaping electronics present in each pixel.
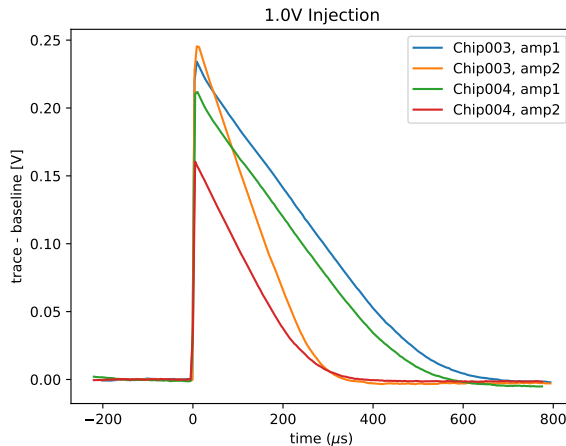
Figure 3: The average of 100 traces from both AstroPix_v1 chips in response to an injected pulse of 1.0 V.

From this study, we can conclude that the probed pixel both respond to the injected charge albeit with different pulse shapes. This builds confidence in the circuitry and response of the chip, as well as data readout, collection, and analysis methods. It also illustrates the degree of variation that can occur in pixel responses. In future AstroPix versions, pixels will be indiviually tuned to limit the variability in pulse shape.

2.3.2 Threshold Measurements

AstroPix requirements define a 25 keV low threshold. This enables the measurement of low-energy astrophysical photons through photoabsorption into a single pixel. In order to measure the threshold of AstroPix_v1 and compare the performance to requirements, a low threshold for data collection must be set such that the sensor is protected from randomly triggering upon noise at an overwhelming rate.

Low-energy depositions from ambient sources (such as fluorescent lighting) or electronics noise are disregarded as background from subsequent analyses with a hard cut on acceptable pulse heights. This defines a low threshold with which measurements are recorded. Compton-scattered deposits within this regime cannot be uniquely identified and are lost. Dedicated runs with no radioactive source and a threshold low enough to trigger upon background hits are used to define the threshold level as that which eliminates all activity from the background runs. This threshold is set on the analog data collecting oscilloscope with millivolt precision. The shape of the resulting background distribution of hits is Gaussian. The amplitude of the response of the analog probed pixels in different chips can differ due to fabrication differences (see Fig. 3). Minimum thresholds of analog signal pulse height for different pixels are shown in Table 2. These threshold values can also be interpreted as energy values after calibration is defined in Section 2.3.3.

Additional background events from Compton-scattered particles from radioactive sources cannot be removed with a hard cut. These are included in subsequent analysis.

2.3.3 Energy Calibration

Charge injection studies of Sec. 2.3.1 validate that AstroPix_v1 responds to signals and fostered the development of software tools, including data collection and analysis. From here, a correlation between AstroPix_v1 response

Table 2: Threshold peak height required for a trace to be considered 'signal' (and not background or noise).

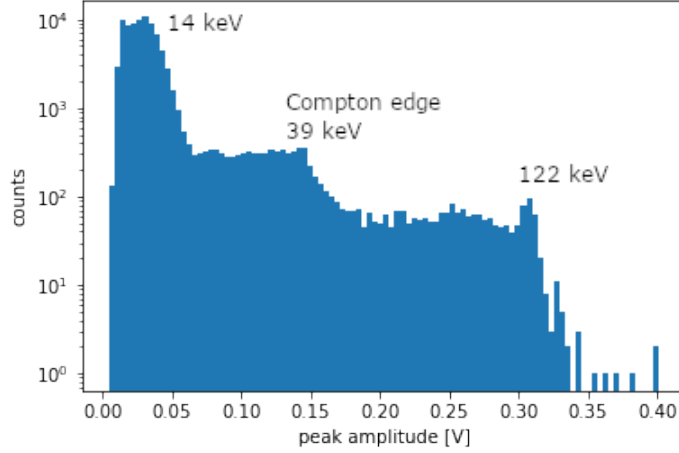| Version	Chip	Pixel	Threshold [mV]	Chip	Pixel	Threshold [mV]
v1	003	amp1	20	004	amp1	10
v1	003	amp2	30	004	amp2	20
v2	1	amp1	60	-	-	-

Figure 4: Spectrum of the raw data collected over 16 hours with AstroPix_v1 chip003 amp1 of Cobalt-57. Photopeaks associated with 14.41 keV and 122.06 keV emission can be seen, as well as a Compton edge at 39.46 keV. Between these features, AstroPix_v1 experiences high background rates from Compton-scattered interactions.

(analog pulse height) and incident particle energy is measured in order to calibrate response spectra into units of energy. Radioactive isotopes with known emission lines were used. The sources utilized in these calibration studies (see Table 3) have emission lines spanning 14 keV - 122 keV. These sources probe the low end of AstroPix's sensitivity regime. Statistics in these studies can be limited due to the radioactivity of the source and the analog readout scheme. Analog data from only one single pixel can be read out during a collection run, leading to a very small sensitive area on the chip. Additionally, the cross section decays with increased photon energy, leading to lower statistics for higher energy incident particles.

Analog data was triggered for readout by the AstroPix_v1 response itself. The height of each response peak is utilized as a proxy for energy deposition. The collection of these signals create spectra of raw data (see Fig. 4) that contain peaks associated with anticipated photopeaks but also high rates of signal recorded between expected peaks. For the remainder of this work, the 30.97 keV photopeak of Barium-133 will be used a particular case study to illustrate raw and calibrated spectra, performance of calibration software, and AstroPix response. Like with Cobalt-57, below the Barium-133 photopeak backscattered signal can also be identified.

The anticipated photopeaks (and single Compton edge) from the raw spectra collected from all the sources in Table 3 are fit with a Gaussian (see Fig. 5 (left) for fitting to Barium-133) where the mean and width are extracted. Due to high background rates, photopeaks are identified and fit using only the five most populated bins. The Compton edge for the 122 keV emission line of Cobalt-57 at 39.46 keV is also considered, and fit with a modified Heaviside function (derivation in 5). The Gaussian mean is used to create a calibration curve (see Fig. 6). The response of AstroPix_v1 to increasing charge is monotonic but not linear and the distribution is

Table 3: Properties of radioactive isotopes used for calibration curve creation. The Compton edge of the Cobalt-57 122 keV photopeak is also considered.

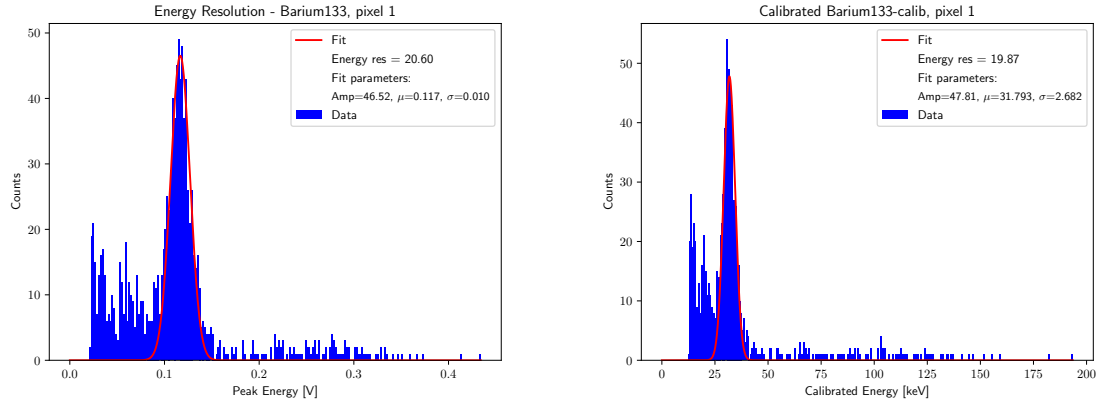| Isotope	Radioactivity [mCi]	Emission Line(s) [keV]
Cobalt-57	0.9973	14.41, 122.06
		39.46
Cadmium-109	1.031	22.16, 88.03
Barium-133	1.05×10^{-4}	30.97
Americium-214	0.1065	59.54

Figure 5: (Left) Gaussian fit to raw data collected with AstroPix_v1 chip003 amp1 of the Barium-133 30.97 keV photopeak over 65 minutes. The Gaussian mean μ is extracted and used to construct a calibration curve. (Right) Barium-133 spectrum from left panel calibrated with third degree polynomial fit, with calibration and test data collected from amp1.
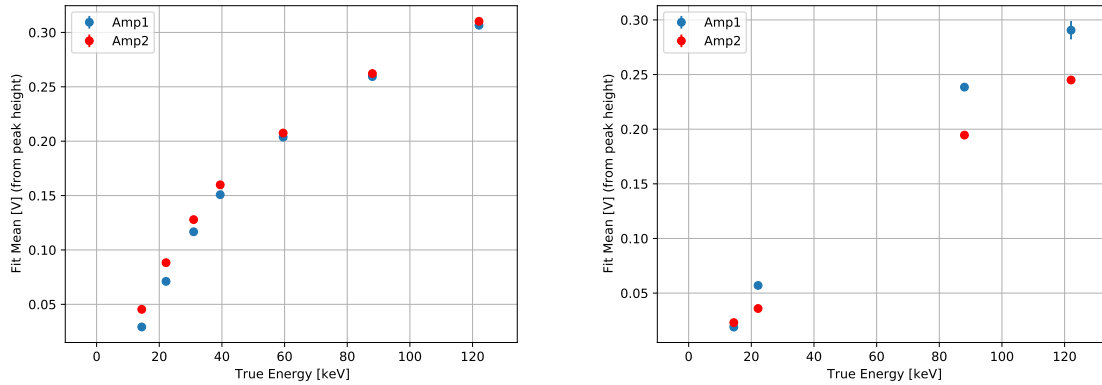

Figure 6: AstroPix_v1 calibration curves for chip003 (left) and chip004 (right). Fewer data points were taken for chip004 due to time constraints, but only four points are required for calibration. Error bars from the error on the fit parameter fall within the diameter of the markers.

best fit with a third-degree polynomial function.

A third degree polynomial describing the relationship between mV and keV the spectra to be calibrated (see Fig. 5 (right)) with all photopeaks falling within 7% of the anticipated value. Though this value does not yet meet AstroPix requirements, it is an impressive start for the first AstroPix design version. The measurement is limited by the analog readout method of data collection from a single $175 \times 175 \ \mu m^2$ pixel. Further improvement can also be expected as data analysis tools continue to develop.

As the photopeak energy increases the energy resolution after calibration decreases (see Fig. 7), indicating higher resolution. Since individual pixel responses differ (as shown in Fig. 3), an individual calibration curve was constructed from data measured from each pixel. Figure 7 (right) illustrates the degredation in performance when a calibration curve derived from a different pixel is used. Figure 5 (right) also illustrates the low energy threshold that AstroPix_v1 can achieve. With the required noise cuts from Table 2, AstroPix_v1 measures signal down to 13 keV.
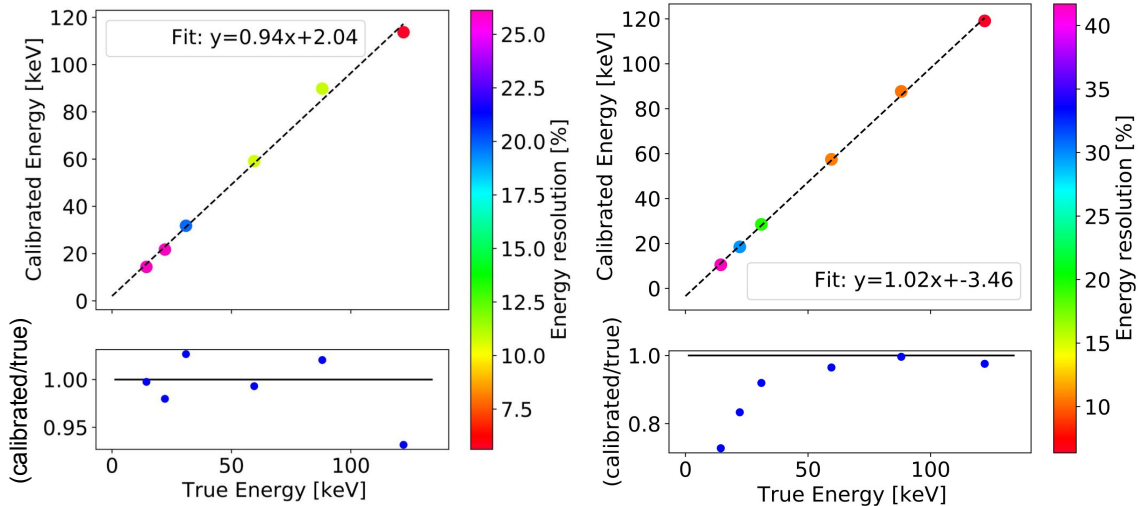
Figure 7: Calibration performance of AstroPix_v1 for all measured photopeaks. Calibration conducted with a third degree polynomial fit using test data collected by chip003 amp1 and calibrated by amp1 (left) and amp2 (right). Calibrating with the same data used to collect test data results in a calibrated mean energy that is closer to the expected value across the entire spectrum, and generally lower energy resolution.

3. ASTROPIX_V2

AstroPix_v2 follows AstroPix_v1 part of the planned incremental design strategy. A key milestone achieved with AstroPix_v2 is the ability to read and record digital data in addition to the analog data investigated with AstroPix_v1 after the implementation of shielding against parasitic capacitance causing comparator oscillations. The results presented in this section consider only analog data in order to draw direct comparisons between ATLASPix and AstroPix_v1. Preliminary digital data conclusions will be presented in Section 5.

3.1 Design Optimization and Setup for AstroPix_v2

Pixel size is one of the incremental changes realized in AstroPix_v2, where the $175{\times}175~\mu\mathrm{m}^2$ pixels of AstroPix_v1 are enlarged to $250{\times}250~\mu\mathrm{m}^2$. An AstroPix_v2 chip is $1{\times}1$ cm^2 and contains a $35{\times}35$ array of these $250{\times}250~\mu\mathrm{m}^2$ pixels.

AstroPix_v2 also features an updated guard ring design around these larger pixels to help control leakage and allow for a higher depletion voltage enabling a deeper depletion depth. By removing unused digital to analog converters (DACs) from the bias block, AstroPix_v2 also sees a reduction of analog power from 14.7 mW/cm^2 to 3.4 mW/cm^2. Previously identified issues with crosstalk from AstroPix_v1 were resolved in AstroPix_v2, and a global timestamp was enabled such that digital signal can be held in buffer during readout and read out with the subsequent trigger.

The test setup for AstroPix_v2 is identical to that of AstroPix_v1, where the chip interfaces with a Nexys FPGA and GECCO board. AstroPix_v2 is also mounted onto a carrier board, so the AstroPix_v1 setup can be reused. Software updates have enabled Python wrappers to facilitate chip configuration and data-taking. Analog data can be collected from 35 pixels (one full row) of AstroPix_v2. This section focuses on the analog response of a single pixel located in the corner of the array.

Like with AstroPix_v1, a bias voltage of -60V is supplied for these measurements. Preliminary studies indicate that maximal depletion of the sensor may occur around -160V, though this may still result in lower depletion than the design requirement of 500 μm. The true depletion depth and optimal bias voltage is still being studied.
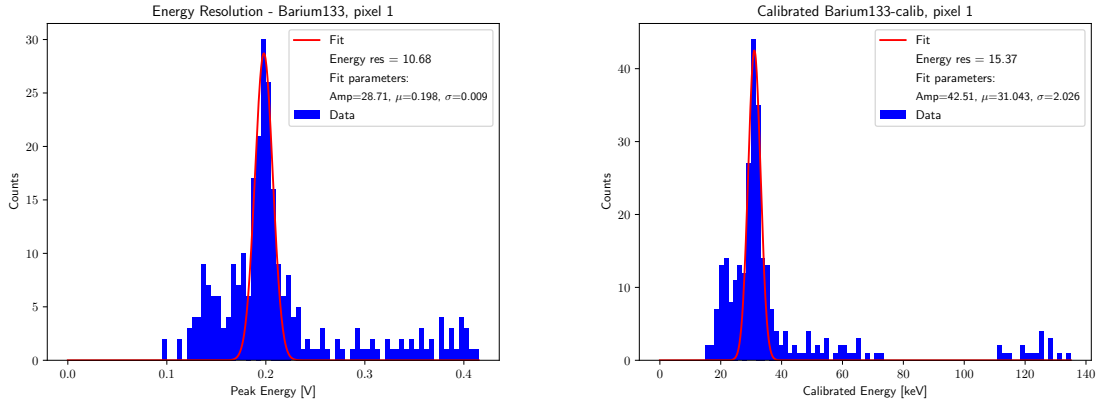
Figure 8: (Left) Gaussian fit to raw data collected with AstroPix_v2 chip1 amp1 of Barium-133 over 5.5 hours. The Gaussian mean μ is extracted and used to construct a calibration curve. (Right) Barium-133 spectrum from left panel calibrated with cubic spline fit, with calibration and test data collected from amp1. The shape of the spectrum changes due to the nonlinearity of the calibration function.

3.2 AstroPix_v2 Characterization Studies

3.2.1 Charge Injection Studies

As with AstroPix_v1, the response of AstroPix_v2 was checked first using an injected charge. Updated DAC settings allow for the shaping of a shorter duration pulse (80 μs vs 600 μs) with a taller peak (0.41V vs 0.24V) than that of Fig. 3. This shape allows for shorter deadtime and less pileup as compared to AstroPix_v1, but also uncovered a limitation in the analog AstroPix_v2 design - an on-chip PMOS source follower saturates at 500 mV, serving as an upper limit to the height of analog pulse that can be collected. This causes the analog response of AstroPix v2 to saturate at energies of 90 keV - a factor of seven less than the required dynamic range of 25-700 keV. This will be resolved in future AstroPix versions, but must be considered in the analysis of AstroPix_v2. This limitation is only present in analog data and does not impact the performance of the digital output.

3.2.2 Energy Calibration

A calibration curve for AstroPix_v2 was made using the response to radioactive isotopes with known emission lines (see Table 3). An identical analysis strategy is used, where spectra of AstroPix_v2 responses (the pulse height) are fit by a Gaussian whose parameters are correlated with anticipated photopeak energies. A higher threshold is required (see Table 2) due to increased electronics noise from the heightened capacitance related to the larger pixels. A spectrum is shown in Fig. 8 (left). Again, note the corresponding increase in measured mean as compared to AstroPix_v1 (see Fig. 5 (left)), yet smaller Gaussian standard deviation. The high rates of backscattered signal below the 30.97 keV photopeak noted in AstroPix_v1 is also decreased in AstroPix_v2 possibly due to a larger distance between the source and the sensor (reducing background from low-energy scattered γ-rays) and/or more complete charge collection due to a larger depletion region.

Like AstroPix_v1, the analog response of AstroPix_v2 to increasing charge is monotonic but not linear. The impact of the PMOS source follower saturation becomes evident around 60 keV and inhibitive around 90 keV as the response pulse height rises more slowly and asymptoticly approaches a value around 400 mV. This impact is large in analog data analysis, however the analog studies presented in this work are intended to serve as a preliminary assessment of the chip's capabilities. Digital readout will be utilized by future AstroPix versions (with a first look presented in Section 5), and it is not impacted by this saturation.

Due to the source follower saturation, the analog calibration curve (see Fig. 9) is best fit with a cubic spline fit. Resulting calibrated spectra (see Fig. 8 (right)) reproduce photopeaks falling within 15% of the anticipated value. This includes the outlying 88 keV photopeak from Cadmium-109. A lack of statistics for the raw spectrum led to poor fitting which propagated to the nonlinearly scaled calibrated spectrum. Without consideration of
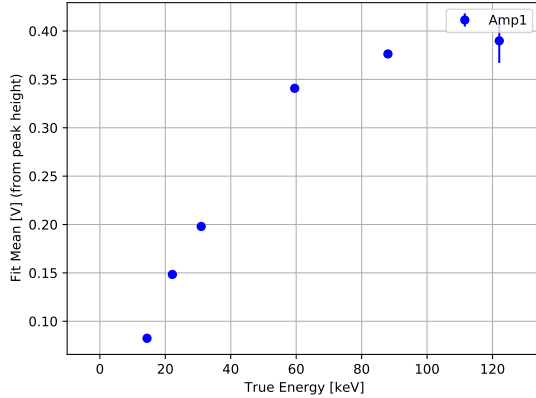
Figure 9: AstroPix_v2 analog calibration curve for chip1. Most error bars fall within the diameter of the markers. The impact of PMOS source follower saturation beginning around 350 mV is evident.
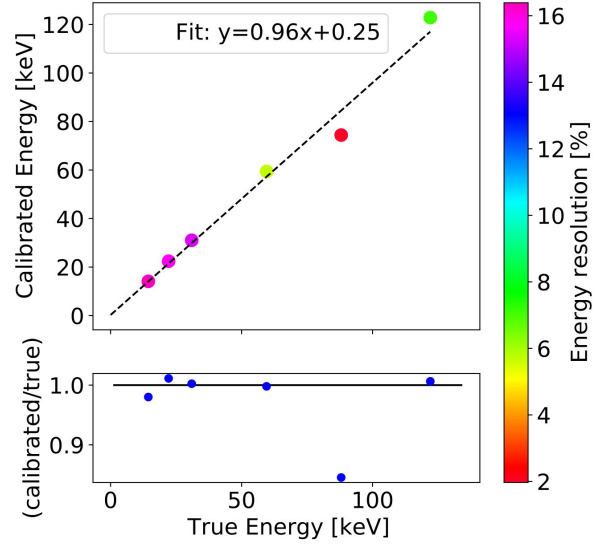

Figure 10: Calibration performance for all tested photopeaks. Calibration conducted with a cubic spline fit using test data collected by chip1 amp1.

this point, the cubic spline calibrations agree with expected values within 3%. This is a vast improvement over AstroPix_v1 calibration, and provides a point of comparison for eventual studies of the digital output. A higher degree of confidence could be placed on a calibration function spanning only from 14 - 60 keV, in the range that AstroPix_v2 is unaffected by source follower saturation. Figure 8 (right) also illustrates that the low energy threshold of 13 keV is consistent with that of AstroPix_v1.

As the photopeak energy increases the energy resolution after calibration also increases (see Fig. 10). Compared to AstroPix_v1 (see Fig. 7), AstroPix_v2 measures a better energy resolution for each calibrated point with $E_{res} < 16\%$ for all points as compared to $E_{res} < 25\%$ with AstroPix_v1.

The case study of the 30.97 keV photopeak of Barium-133 is considered in Table 4. Analog measurements from AstroPix_v2 perform better than those from AstroPix_v1, and the planned incremental upgrades to AstroPix design is delivering results consistently closer to design requirements and with higher precision. It is assumed that the final AstroPix design will be dominated by electronics noise from the range of 25-122 keV with a constant energy resolution of 5 keV RMS. Therefore the required energy resolution performance at 30.97 keV of 38% is already being met with analog measurements made in the lab of all tested AstroPixversions. It must be noted, though, that the presented measurements are the result of analog measurements of a single, well-characterized pixel and ultimate performance of AstroPix must be judged on the digital performance of the full array.

The lowest measured energy resolution with ATLASPix is also included in Table 4, although the thinner ATLASPix wafer is easier to fully deplete and was previously optimized by the ATLASPix team for measurement while AstroPix characterization and optimization is occurring in tandem.

When considering calibration as a whole, AstroPix_v2 experiences limitations in its calibration power due largely to the PMOS source follower saturation at 500 mV. The effective range of calibration from 0-60 keV is more limited than that of AstroPix_v1 which could successfully calibrate up to 122 keV. However, measured points within this valid range were better calibrated with AstroPix_v2 as compared to AstroPix_v1. This effect is noted and will improve with updated hardware in future AstroPix iterations, however a shift from analog data to digital data will also limit the scope of this setback. Digital data, not analog data, will be utilized exclusively in the final AstroPix design so shortcomings in the analog circuitry (used at this stage for testing) do not necessarily inhibit the overall intended chip performance.

4. RADIATION TESTING

Preliminary testing of AstroPix_v2 has been conducted in two separate beam environments. The intention of this testing is to raise the technology readiness level (TRL) of AstroPix and increase confidence in the chip's capabilities on orbit. Results presented here are preliminary, and currently undergoing independent assessment.

AstroPix_v2 participated in two campaigns at the Fermilab Test Beam Facility (Ref. 6) where it was exposed to a 300 kHz 120 GeV proton beam. Both the digital and analog performance was assessed in these qualitative tests. AstroPix_v2 was able to register and record signals in this high-energy and high-flux environment, though the rate of interaction is much greater than the environment AstroPix is designed for in orbit. This high rate overwhelmed the current software designed for debugging and chip characterization, which optimized for lower rates of <5 Hz and is not the final flight-ready version. None of the monitored power rails increased current draw during beam running as compared to bench running. These successful tests were the first radiation tests of any AstroPix chip and serve as an important milestone for the continued development of the technology.

AstroPix_v2 was also subjected to radiation testing at the 88-Inch Cyclotron operated in conjunction with the Berkeley Accelerator Space Effects facility at Lawrence Berkeley National Laboratory (Ref. 7). Here, heavy ions ranging from Argon to Xenon with an atomic tune of 16 MeV/(atomic mass unit) illuminated AstroPix_v2. The susceptibility to latchup was first recorded. This is a state of inactivity in which an incident ion deposits significant charge in a pixel, inducing a perpetually open transistor and leading to runaway current draws. The latchup state must be corrected through a chip reset and reconfiguration. The sensor successfully survived this test, withstanding a fluence (integrated flux) of 1×10^7 particles/cm^2 at an effective linear energy transfer (LET) of 65 MeV*cm^2/mg.

Testing for single event functional interrupts (SEFI) was also conducted. This event may occur when a heavy ion collision interacts with the digital periphery and flips a bit upon readout causing data degradation or corrupted configuration. Proper operation can be restored with a chip reset or reconfiguration as no permanent damage is sustained. Possible evidence of SEFIs with an onset of LET=22.5 MeV*cm^2/mg were noted during the run, identifying elements of the digital framework of the chip that may be susceptible. This informed an updated design of future AstroPix versions, which can limit the onset of SEFIs to higher LET values.

5. FUTURE PLANS AND SUMMARY

The digital output of AstroPix_v2 is still being tested, and will be included in a dedicated paper. The previously considered analog data is the signal pulse returned from a single pixel. For digital output, this pulse is digitized on chip and a bitstream with encoded hit information is read out. A particle interaction in a pixel will cause the pixel's comparator to trigger. The comparator also calculates a Time over Threshold (ToT) value associated with the particle interaction. This is a true time in microseconds that the response pulse exceeded a defined threshold value. This ToT value, rather than pulse height as seen in the analog case, serves as a proxy for the amount of charge deposited. A larger ToT value indicates a larger charge deposition. The threshold value used to calculate the ToT is universal for every pixel across the chip and in AstroPix_v2 cannot be set on a pixel-by-pixel basis. All comparator readings from the full array are OR'd into one channel containing row hit information and another of column hit information. The triggering of any comparator will impact an interrupt signal which indicates that the full chip should be read out.

Table 4: Comparison of AstroPix measurements with ATLAPix performance and AstroPix requirements. AstroPix energy resolution requirement is 5 keV RMS at 122 keV which is assumed to be constant down to 25 keV, or a 38% energy resolution at 30.97 keV. Energy resolution values are stated with respect to the FWHM. The 500 μm wafer requirement represents the depletion depth requirement.

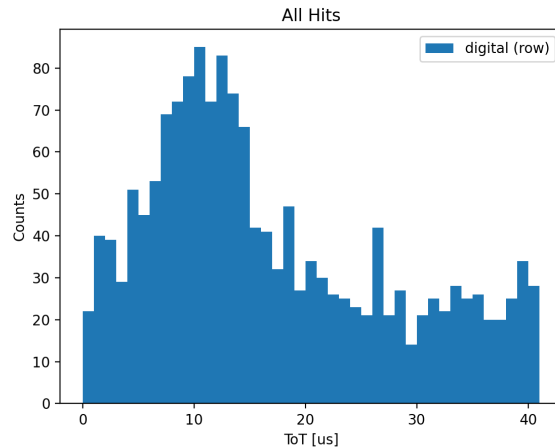|	Energy Resolution at 30.97 keV [%]	Wafer Thickness [μm]
Requirement	38%	500
ATLASPix	7.3 ± 1.2	100
AstroPix_v1	19.9 ± 7.4	700
AstroPix_v2	15.4 ± 2.9	700

Figure 11: Preliminary spectrum of digital data recorded over 3 hours from one AstroPix_v2 pixel with a Barium-133 source.

Preliminary work shows that the sensor is able to trigger upon, read out, and decode data (see Fig. 11). A clear photopeak in response to a Barium-133 source can be seen in this ToT spectrum when data from a single digital pixel is read out. This early work is intended to serve as an illustration that digital data can be collected and interpreted, and not yet serve as an indication of AstroPix_v2 digital performance. Work is currently underway to further understand the performance of the digital readout system with studies planned to map noise and gain variations between pixels, record digital signals from more pixels on the array, and optimize the comparator's threshold value.

AstroPix_v3 was submitted for fabrication in Summer 2022. Additional power-reducing improvements will be incorporated into the design with a target total draw of < 1mW per cm^2. The pixel size will also continue to increasing in AstroPix_v3, up to 500×500 μm^2. Within this pixel pitch, the active area will be 300×300 μm^2 and the total array will increase to 2×2 cm^2. This additional space allows for the removal of conductive p-wells between pixels, limiting noted leakage of the charge cloud into the array periphery. AstroPix_v3 will also be designed with the possibility to dice the wafer into a quad-chip - four individual chips cut from the wafer as one 4×4 cm^2 square of identical MAPS chips, quadrupling the number of pixels. This is the unit that will act as a building block for larger structures such as a future telescope tracker. Readout capability of the quad chip involving daisy-chaining the signal from one chip through the others on SPI readout was implemented in AstroPix_v2, but will be fully tested in AstroPix_v3. With this full quad-chip, environmental testing of of AstroPix_v3 in a space environment is also planned with the development of a four-layer hosted payload to be included on a sounding rocket mission. The success of this testing will further raise the TRL. In AstroPix_v4, digital state triplication will be introduced to protect the chip against single event functional interrupts possibly observed in the radiation testing discussed in Sec. 4.

In summary, AstroPix is a CMOS MAPS chip designed for the space environment. A robust design and characterization strategy is in place to advance the technology from its current stage to flight readiness. The current version under test, AstroPix_v2, is capable of analog and digital readout and a comprehensive analysis of the analog response has been presented and compared to the performance of the previous version, AstroPix_v1. Metrics such as total power draw do not yet meet AstroPix design requirements, but the AstroPix design strategy relies upon incremental changes between versions building to the final design. Therefore, the consistent improvement of performance in updated versions is a success toward realizing a final AstroPix. The utilization of AstroPix in future γ-ray telescopes (such as AMEGO-X, as described in Ref. 8) will enable high energy, angular, and position resolution for low power consumption these next-generation detectors.

ACKNOWLEDGMENTS

REFERENCES

[1] Brewer, I., Negro, M., Striebig, N., Kierans, C., Caputo, R., Leys, R., Peric, I., Fleischhack, H., Metcalfe, J., and Perkins, J., "Developing the future of gamma-ray astrophysics with monolithic silicon pixels," *Nucl. Instrum. Meth. A* **1019**, 165795 (2021).

[2] Perić, I. and Berger, N., "High Voltage Monolithic Active Pixel Sensors," *Nucl. Phys. News* **28**(1), 25–27 (2018).

[3] Schöning, A., Anders, J., Augustin, H., Benoit, M., Berger, N., Dittmeier, S., Ehrler, F., Fehr, A., Golling, T., Sevilla, S. G., Hammerich, J., Herkert, A., Huth, L., Iacobucci, G., Immig, D., Kiehn, M., Kröger, J., Meier, F., Gonzalez, A. M., Miucci, A., Noehte, L. O. S., Peric, I., Prathapan, M., Rudzki, T., Schimassek, R., Sultan, D., Vigani, L., Weber, A., Weber, M., Wong, W., Zaffaroni, E., and Zhangh, H., "Mupix and atlaspix – architectures and results," (2020).

[4] Striebig, N., *Development of Integrated Sensors for Gamma Ray Astronomy*, Master's thesis, Karlsruhe Institute of Technology (2021).

[5] Safari, M. J., Davani, F. A., and Afarideh, H., "Differentiation method for localization of compton edge in organic scintillation detectors," (2016).

[6] "Fermilab test beam facility." https://ftbf.fnal.gov/. Accessed: 2022-07-20.

[7] McMahan, M., "Radiation effects testing at the 88-inch cyclotron," in [*1999 Fifth European Conference on Radiation and Its Effects on Components and Systems. RADECS 99 (Cat. No.99TH8471)*], 142–147 (1999).

[8] Fleischhack, H., "AMEGO-X: MeV gamma-ray Astronomy in the Multi-messenger Era," in [*Proceedings of 37th International Cosmic Ray Conference — PoS(ICRC2021)*], **395**, 649 (2021).